



Ionically self-assembled terephthalylidene-bis-4-*n*-alkylanilines/*n*-decanesulfonic acid supramolecules: Synthesis, mesomorphic behaviour and optical properties

Agnieszka Iwan^{a,*}, Henryk Janeczek^a, Patrice Rannou^b

^a Centre of Polymer and Carbon Materials, Polish Academy of Sciences, 34 M Curie-Skłodowska Street, 41-819 Zabrze, Poland

^b Laboratoire d'Electronique Moléculaire, Organique et Hybride, UMR5819-SPRAM (CEA-CNRS-University J. FOURIER-Grenoble I), DRFCM, CEA-Grenoble, 17 Rue des Martyrs, 38054 Grenoble Cedex 9, France

ARTICLE INFO

Article history:

Received 9 May 2008

Received in revised form 19 August 2008

Accepted 20 August 2008

Keywords:

Azomethines

Protonation

Liquid crystalline

Photoluminescence

ABSTRACT

This paper describes the preparation, mesomorphic and photophysical studies of a two type of calamitic molecules derived from azomethines, *N,N'*-(1,4-phenylenebis(methan-1-yl-1-ylidene)bis(4-pentylbenzenamine) (LCBAZ1) and *N,N'*-(1,4-phenylenebis(methan-1-yl-1-ylidene)bis(4-decylbenzenamine) (LCBAZ2) before and after protonation with the *n*-decyl sulfonic acid (DSA). The lengths of the outer spacers are four or nine methylene units connected with the imine group by phenyl ring in the para position. Liquid crystal properties of the undoped and doped azomethines are studied by differential scanning calorimetry (DSC) and polarizing optical microscopy (POM). Wide-angle X-ray diffraction (WAXD) technique is used to probe the structural properties of the azomethines as well as its complexes. The lengths of the outer flexible spacers have an effect on the mesomorphic properties of the azomethines. The compound LCBAZ2 with nine methylene units exhibit smectic phases (Sm C and Sm X), while the LCBAZ1 with four methylene units exhibit nematic and smectic phases (N and Sm C). The effects of protonation on the phase transitions of the azomethines are investigated. The structure formation of (LCBAZ_x)₁(DSA)₂ complexes are discussed on the basis of FTIR spectroscopy. Additionally, the azomethines before and after protonation with DSA are investigated by UV–vis and photoluminescence (PL) spectroscopy. With the exception of LCBAZ1 in its undoped state, the chloroform solution of the doped or undoped azomethines exhibit greenish fluorescence when the solutions are subjected to 400 nm excitation wavelength. It are concluded that the combination of the molecular and supramolecular engineering concepts stabilized the smectic phase.

© 2008 Elsevier B.V. All rights reserved.

1. Introduction

Various kinds of molecular interactions such as hydrogen bonds, halogen bonds and electrostatic interaction are widely used to assemble the ordered supramolecular structures [1–4]. Interactions between the polymer (oligomer) chains and dopant (i.e. Lewis and Brønsted acids) influence changes of the electrical, optical, thermal and mechanical properties in comparison with the undoped compound and also improve solubility [1].

Azomethines (polyazomethines) belong to the classic type of molecules with liquid crystalline (LC) properties [1,5–15]. For example, Henderson et al. [10] characterized a series of semi-flexible LC tetramers with the two azomethine (HC=N–), two azo

(–N=N–) bonds and aliphatic spacers. All the tetramers exhibited an enantiotropic nematic phase. While Smith et al. [13] obtained the azomethines based on fluorinated carbon chains exhibited nematic and smectic A phase transitions.

Less attention is paid to the LC oligomers with the azomethine bond after doping, especially after protonation [16,17]. So far, one important property of the azomethines is fact that lone electrons pair of nitrogen atom in the imine group (HC=N–) is able to form supramolecular interactions with many electrophiles (dopants) [1–4]. Pucci et al. [16] studied the liquid crystalline azomethine before and after protonation with 4-decyloxybenzoic acid, being able to form H-bond with pyridyl moiety of the azomethine. The azomethine complexes exhibited nematic and smectic C phase transitions.

Also a lot of works is dedicated to investigate the liquid crystalline properties of the terephthalylidene-bis-4-*n*-alkylanilines [18–31] especially by X-ray technique. However, in accordance with the best our knowledge the LC behaviour as well as photolumines-

* Corresponding author. Tel.: +48 32 2716077; fax: +48 32 2712969.
E-mail address: agnieszka.iwan@cmpw-pan.edu.pl (A. Iwan).

cence properties of terephthalylidene-bis-4-*n*-alkylanilines after protonation were not investigated so far.

The main goal of this paper is obtain ionically self-organized thermotropic liquid-crystalline comb-shaped supramolecules via protonation of the imine sites by special protonating agent. All compounds after protonation with *n*-decyl sulfonic acid (DSA) formed smectic phase. This is probably the first example of the azomethine-based derivatives exhibiting LC properties after protonation with the DSA. Their fluorescent properties were also examined as potential application in the opto(electronics).

2. Experimental

2.1. General

All chemicals and solvents were of reagent grade obtained from Aldrich Chemical Co., and all solvents were dried by standard techniques. The synthesized compounds in the undoped state were characterized by ^1H and ^{13}C NMR and elemental analysis. Undoped compounds were also characterized by Fourier transform infrared (FTIR) and ultraviolet-visible (UV-vis) absorption and photoluminescence (PL) spectroscopy. Azomethines doped with DSA were subjected to UV-vis and PL spectroscopy. NMR was recorded on a Varian Inova 300 MHz Spectrometer. Chloroform *d* (CDCl_3) containing TMS as an internal standard were used as solvent. Elemental analyses (C, H, N) were carried out by the 240C PerkinElmer analyser. FTIR spectra of the azomethines were recorded on a PerkinElmer paragon 500 spectrometer (wavenumber range: 400–4000 cm^{-1} ; resolution: 2 cm^{-1}). Solution (CHCl_3) UV-vis absorption spectra were recorded on Hewlett-Packard 8452A spectrophotometer. Photoluminescence measurements of the azomethines were carried out on a Jobin-Yvon HR 460 monochromator equipped with a CCD silicon detector cooled at 140 K. Excitation was performed with an argon laser at 400 nm (1.25×10^{-3} M). Melting point and liquid crystal properties of the synthesized compounds were determined by differential scanning calorimetry (DSC) on a TA-DSC 2010 apparatus using sealed aluminium pans under nitrogen atmosphere. X-ray diffraction patterns were recorded using powder or film samples on a wide-angle HZG-4 diffractometer working in typical Bragg geometry. Cu K α radiation was applied.

2.2. General synthetic procedure of LCBAZx

A detailed procedure is following: a solution of terephthalaldehyde (TA) (1.0 mmol) in 5 ml of *N,N*-dimethylacetamide (DMA) was added to a solution of amine (2.0 mmol) in DMA (5 ml) with 0.06 g of *p*-toluenesulfonic acid (PTS). The mixtures were introduced into a 20-ml, two-necked, round-bottomed flask equipped with an overhead stirrer, a reflux condenser and an argon inlet. The mixture was refluxed with stirring for 10 h. Then the compound was filtered, washed and dried at 60 °C under vacuum for 12 h, and finally crystallised from a methanol.

2.2.1. *N,N'*-(1,4-Phenylenebis(methan-1-yl-1-ylidene)bis(4-pentylbenzenamine) (LCBAZ1)

Yellow powder, yield: 88%. ^1H NMR (300 MHz, CDCl_3 , TMS) [ppm]: δ = 8.52 (s, 2H, 2 × HC=N); 7.98 (4H, s, 4 × H_{Ar}); 7.19–7.21 (m, 8H, 8 × H_{Ar}); 2.60–2.63 (m, 4H, 2 × CH₂); 1.32–1.36 (m, 4H, 2 × CH₂); 1.61–1.64 (m, 4H, 2 × CH₂); 0.90–0.92 (m, 6H, 2 × CH₃). ^{13}C NMR (75 MHz, CDCl_3 , TMS) [ppm]: δ = 158.55, 149.24, 141.46, 138.61, 129.98, 128.96, 120.87, 35.46, 31.46, 31.18, 22.53, 14.03. Anal. Calcd. for $\text{C}_{30}\text{H}_{36}\text{N}_2$: C, 84.86%; H, 8.55%; N, 6.60%. Found: C, 84.92%; H, 8.61%; N, 6.80%. mp: 150 °C. FTIR (KBr): 2951, 2923, 2854, 1623,

1598, 1562, 1499, 1467, 1419, 1364, 1303, 1192, 1171, 1116, 1013, 970, 884, 852, 839, 812, 728, 591, 566, 551 cm^{-1} .

2.2.2. *N,N'*-(1,4-Phenylenebis(methan-1-yl-1-ylidene)bis(4-decylbenzenamine) (LCBAZ2)

Yellow powder, yield: 84%. ^1H NMR (300 MHz, CDCl_3 , TMS) [ppm]: δ = 8.53 (s, 2H, 2 × HC=N); 7.99 (4H, s, 4 × H_{Ar}); 7.17–7.24 (m, 8H, 8 × H_{Ar}); 2.60–2.65 (m, 4H, 2 × CH₂); 1.61–1.63 (m, 4H, 2 × CH₂); 1.27–1.31 (m, 28H, 14 × CH₂); 0.86–0.90 (m, 6H, 2 × CH₃). ^{13}C NMR (75 MHz, CDCl_3 , TMS) [ppm]: δ = 158.57, 149.24, 141.38, 138.62, 129.15, 128.98, 120.87, 35.52, 31.89, 31.52, 29.61, 29.60, 29.51, 29.32, 29.29, 22.68, 14.12. Anal. Calcd. for $\text{C}_{40}\text{H}_{56}\text{N}_2$: C, 85.05%; H, 9.99%; N, 4.96%. Found: C, 85.05%; H, 9.82%; N, 5.10%. mp: 70 °C. FTIR (KBr): 3031, 2955, 2916, 2847, 1623, 1600, 1594, 1498, 1467, 1415, 1358, 1303, 1261, 1197, 1170, 1116, 1100, 1013, 971, 938, 906, 888, 848, 831, 819, 783, 720, 557, 529 cm^{-1} .

2.3. Protonation of azomethines

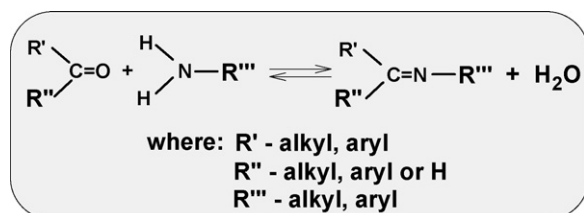
Protonation of the azomethines with the DSA was carried out at room temperature using chloroform as a solvent. DSA was added to the chloroform solution of the azomethines studied in the 1:1 ratio with respect to the imine nitrogens.

3. Results and discussion

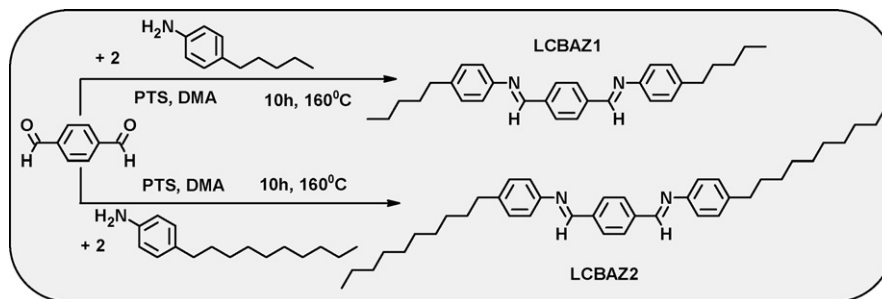
3.1. Synthesis and characterization

The synthetic route for the azomethines is quite straightforward, and each reaction step is a relatively well-known type. The most common method for the imine synthesis is the reaction of carbonyl group in the aldehyde or ketone with the amine being usually acid catalysed. The synthetic pathway for the imines is summarized in Scheme 1. This reaction was first described by Schiff in 1864 and because of this imines are often referred to as Schiff bases [32]. If *R'* is a hydrogen atom, i.e. the reacting group is the aldehyde one product of the condensation sometimes is called aldimine or azomethine while in the case when *R'* exhibits alkyl or aryl structure, i.e. the reacting group is the ketone—the corresponding compound after condensation with the amine is called ketimine or ketanil.

Imine bond formation is a simple reaction which involves loss of H_2O within a single molecule, or between two molecules containing amino and carbonyl groups, such that a C=N double bond is formed either intra- or inter-molecularly [33]. The reaction, which is acid-catalysed, is executed typically by refluxing the starting materials under azeotropic conditions. Many external considerations, including solvent, concentration, pH and temperature, as well as steric and electronic factors, can influence the equilibrium shown in Scheme 1. As such, there are many parameters that can be altered in order to drive the reaction forward—or indeed backwards. For a dynamic reaction, like imine bond formation, to proceed in the direction of products, i.e. imines, the change in the free energy dur-



Scheme 1. Schematic reactions of the imine structure formation.



Scheme 2. Chemical structure of the synthesized azomethines.

ing the reaction must be favourable, i.e. ΔG° in Eq. (1) must be less than zero:

$$\Delta G^\circ = \Delta H^\circ - T\Delta S^\circ \quad (1)$$

Azomethines described in this paper were prepared from the terephthalaldehyde (TA) and two amines via high temperature solution condensation in *N,N*-dimethylacetamide (DMA) at 160 °C (see Section 2). Substrates were introduced into a 20-ml, two-necked, round-bottomed flask equipped with an overhead stirrer, a reflux condenser and an argon inlet. Azomethines yield was in the range of 84–88% in dependence on the amines structures (see Section 2). The compounds were soluble at room temperature in chloroform, THF, DMA, and HMPA. The azomethines were characterized by FTIR, proton and carbon NMR spectroscopy and elemental analysis. The synthetic pathway along with chemical structures of the azomethines synthesized in this research is presented in Scheme 2 whereas their principal spectroscopic and molecular characteristics are collected in Section 2. The spectral data were in accordance with the expected formula.

In Section 2 NMR data concerning two compounds investigated are collected. In particular the signal about 159 ppm, present in the ^{13}C NMR spectra of the compounds, confirms the existence of the azomethine group carbon atoms. In proton NMR spectra of the investigated compounds the imine proton signal at 8.52 ppm was observed. ^1H and ^{13}C NMR spectra of the LCBAZ1 and LCBAZ2 are present in Fig. 1.

3.2. Protonation of azomethines

The main aim of this paper is preparation new types of luminescent, amphiphilic, supramolecular compounds in which the lateral groups are bonded to the π -conjugated main chain not by covalent bonds as it has been done to date but by ionic-type bonds. This ionically bonded lateral group must serve as dopant anions which strongly influence not only the processibility but also the band structure, and by consequence the spectroscopic properties, of the compounds. This approach requires a careful design of the dopant structure which promotes supramolecular ordering of the systems by molecular recognition phenomena. We propose an unique approach in which the processibility, supramolecular structure and by consequence selected physical properties of the electroactive compounds will be tuned via specific interactions with specially designed functional dopant capable of inducing a controlled order in the host compound. Proposed schematic model for the interaction between the azomethines and the protonating agent are presented in Scheme 3.

Protonation of the azomethines with the DSA was carried out at room temperature using chloroform as a solvent. DSA was added to the chloroform solution of the azomethines studied in

the 1:1 ratio with respect to the imines nitrogen in order to assure full protonation of the compound. Azomethines doped with the DSA were subjected to DSC, POM, FTIR, UV-vis and PL spectroscopy.

This paper reports the first example of the use of DSA to modified liquid crystalline properties as well spectroscopic (FTIR) and optical (UV-vis, PL) properties of the liquid crystalline azomethines with odd- and even-aliphatic chain. In our previous paper [36] we described the spectroscopic and optical properties, mainly UV-vis and FTIR of doped with DSA polyketimine obtained from 3,8-diamino-6-phenylphenanthridine and *trans*-1,2-dibenzoyl ethylene (PK1). The absorption spectrum of the doped with DSA PK1 exhibited the small red shift (5 nm) in the position of ketimine band in UV-vis spectrum in DMA solution. In FTIR spectrum of doped PK1 the area of band attributed to stretching vibrations of ketimine group diminishes a little, while the band at about 1625 cm^{-1} ascribed to stretching vibrations of phenanthridine ring disappears. This indicates that DSA in the case of PK1 interact mainly with nitrogen lone electron pair of phenanthridine ring [36].

The synthesis and characteristic of the DSA will be present in the separate paper [37].

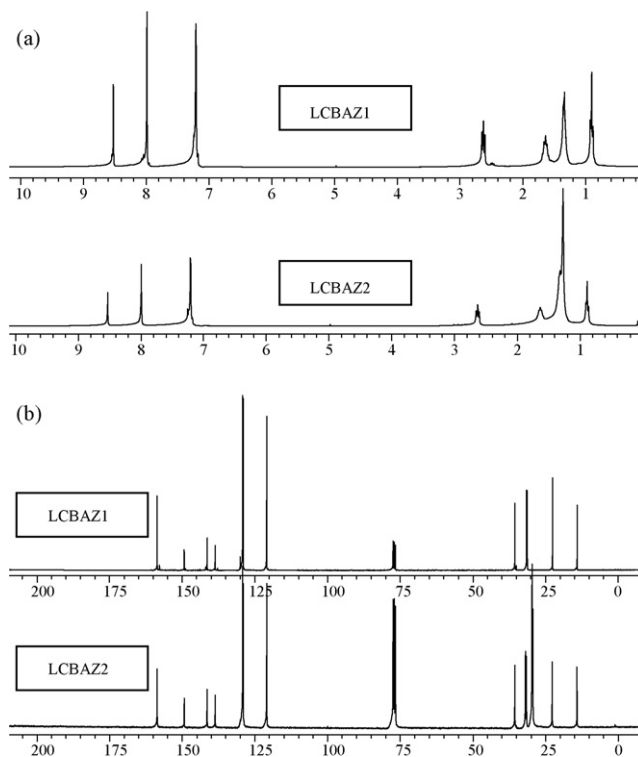
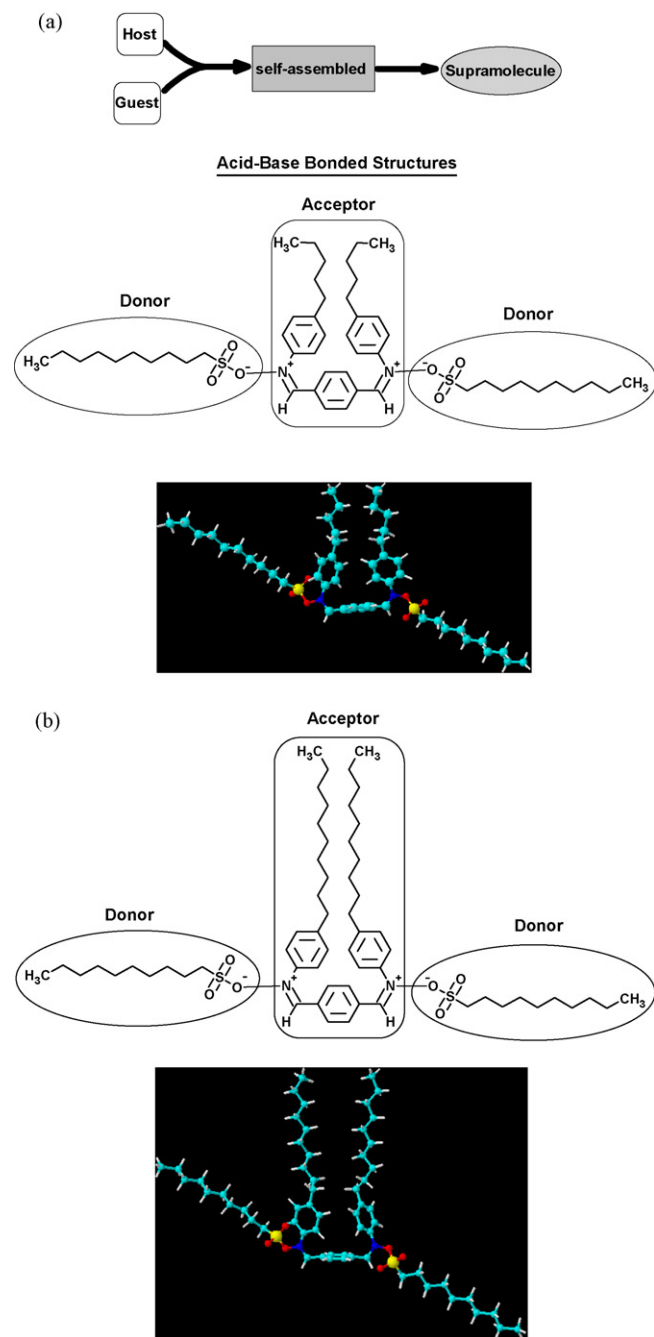


Fig. 1. (a) ^1H NMR and (b) ^{13}C NMR spectra of the azomethines.



Scheme 3. Proposed schematic model for the interaction between the azomethine and protonating agent.

3.3. FTIR spectroscopy

In the FTIR spectra, the absorption band at about 1623 cm^{-1} for the LCBAZ1 and LCBAZ2, which is characteristic of the -HC=N- group, confirms the presence of the azomethine group. In addition to the -HC=N- stretching band, a band at 1596 cm^{-1} can be distinguished ascribed to the C=C stretching deformations in the aromatic ring. Small changes are observed for the vibrations that originated from the alkyl chain. The stretching vibration bands of the alkyl spacer appeared at 2923 and 2854 cm^{-1} for the LCBAZ1 and at 2916 and 2847 cm^{-1} for the LCBAZ2 (see Fig. 2a).

The vibration bands of the alkyl spacer can be assigned to the antisymmetric and symmetric CH_2 vibration. It is known that

the frequencies of the bands due to the CH_2 antisymmetric and symmetric modes of the alkyl chain usually appear at 2915 and 2850 cm^{-1} , corresponding to highly ordered hydrocarbon chains with an all-trans conformation [34,35]. All of the CH_2 antisymmetric vibration in the case of the LCBAZ1 appeared at a relatively higher frequency, indicating the existence *trans* and *cis* isomers in the hydrocarbon chains. While for the LCBAZ2 only the hydrocarbon chains with an all-trans conformation were found.

FTIR spectroscopy provides a facile method of elucidating the effect of Brønsted acid protonation on the molecular structures of the azomethines. LCBAZ1 and LCBAZ2 with the DSA (dopant) at 1:2 ratio was dissolved in chloroform and after evaporating of the solvent at vacuum FTIR spectra were recorded. In the region characteristic for the stretching vibrations of HC=N- group FTIR spectra of the doped samples investigated differ from this of the undoped ones (Fig. 2b–d). It can be mentioned that chosen protonation agent have no bands in that region. The most evident changes can be noticed for the imine band of the azomethines doped with the DSA. In that case the broadening of the imine band along with shift of absorption to shorter wavelength is recorded. Simultaneously the other bands corresponding to stretching vibrations of the imine band decrease their areas (Fig. 2d). On the other hand changes are also observed for the bands corresponding to the stretching vibrations of the aliphatic spacers of the doped compounds. The band at 2923 cm^{-1} associated with the aliphatic group asymmetric stretching vibrations at LCBAZ1 doped with the DSA spectrum is shift to the shorter wavelength for the doped LCBAZ1. The band at 2854 cm^{-1} ascribed to symmetric stretching vibrations of the aliphatic group of the undoped LCBAZ1 is shift to the shorter wavelength for the doped LCBAZ1 (see Fig. 2b). On the other hand the band at 2847 cm^{-1} (undoped LCBAZ2) is shift to the longer wavelength for the doped LCBAZ2, while the bands at 2916 and 2955 cm^{-1} are not change for the doped compound (see Fig. 2c).

3.4. Mesomorphic properties

The mesomorphic behaviour of the compounds was studied by DSC and POM. The phase transitions and thermodynamic data of the undoped and doped compounds are summarized in Tables 1 and 2.

The mesomorphic results indicated that the compound LCBAZ1 showed nematic and smectic mesophases, while the compound LCBAZ2 showed only smectic mesophases. As can be seen from Tables 1 and 2, the formation of the mesophases observed was strongly dependent on the length of the side chains. Upon DSC analysis all compounds exhibited typical transition behaviour, and two enantiotropic transitions, crystal-to-mesophase (Cr/M) and mesophase-to-isotropic (M/I), were observed. Both the melting temperatures and the clearing temperature slightly decreased with increase the length of the side chains, i.e. 48 (LCBAZ1) $<$ 51 (LCBAZ2) and 230.6 (LCBAZ1) $>$ 181.5 (LCBAZ2) on cooling cycle. Also the temperature range of the mesophases was decreased with increase the length of side chains. The DSC analysis of the compounds LCBAZ1 and LCBAZ2 showed four an endothermic clearing transition on the second heating cycle. When cooled from the isotropic liquid state to room temperature, the compounds exhibited three or five exotherms corresponding to the transition from the isotropic liquid to crystalline phase (see Fig. 3).

Compound LCBAZ2 showed a crystal to isotropic liquid transition at $183.4\text{ }^\circ\text{C}$ with a $\Delta H = 13\text{ J/g}$ on the second heating cycle. On cooling from the isotropic state to room temperature, a small exothermic peaks appeared at 181.5 and at $146.7\text{ }^\circ\text{C}$ with a $\Delta H = 13$ and 8.6 J/g , respectively, corresponding to the transition from the isotropic liquid to the liquid crystalline phase. Compound LCBAZ1 has isotropisation at higher temperature being observed at 230.8 and at $230.5\text{ }^\circ\text{C}$ on heating and cooling of the sample, respectively.

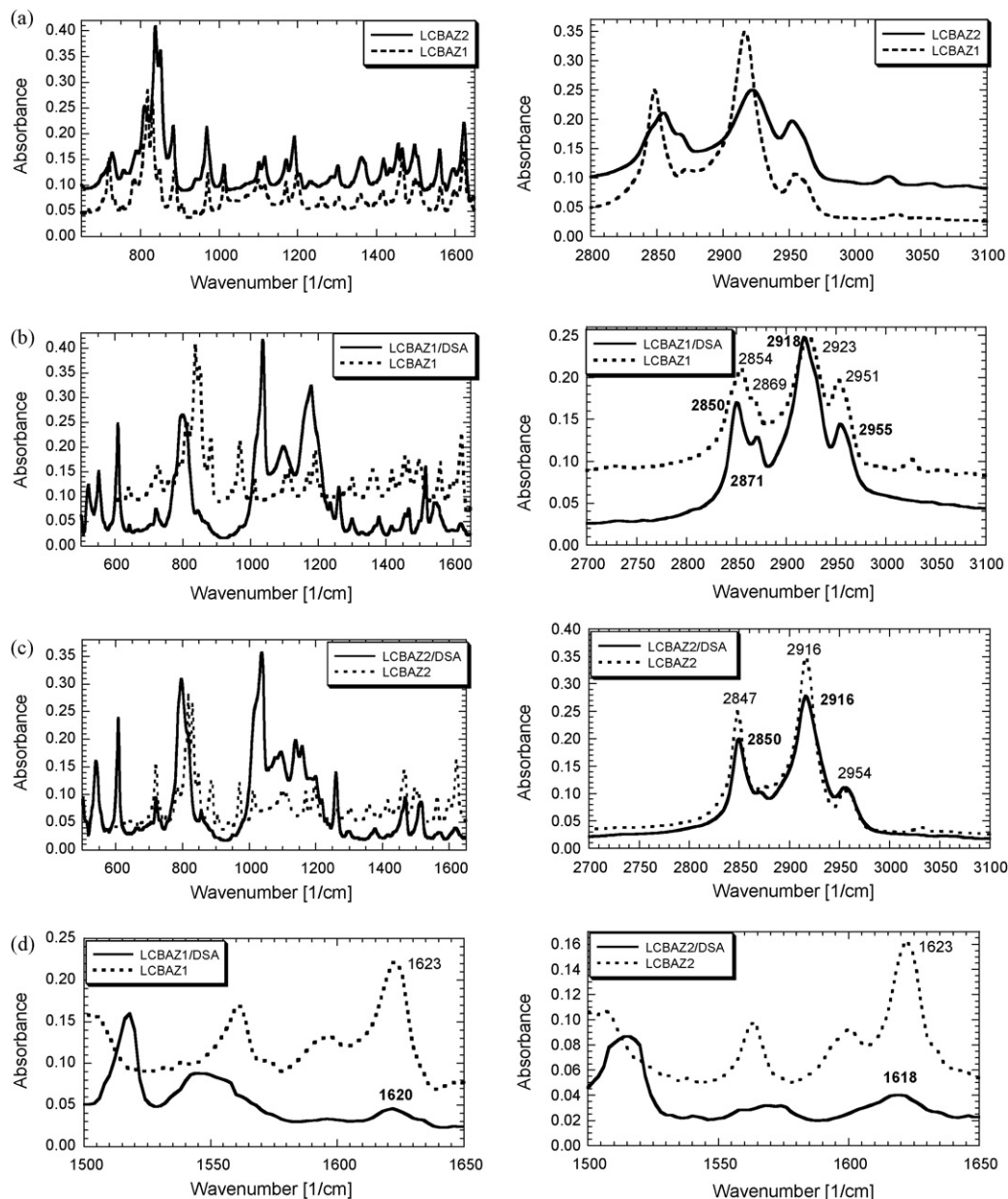


Fig. 2. FTIR spectra of: (a) undoped azomethines in the range of 600–1650 cm^{-1} and 2800–3100 cm^{-1} , (b) doped LCBAZ1 in the range of 500–1650 cm^{-1} and 2700–3100 cm^{-1} , (c) doped LCBAZ2 in the range of 500–1650 cm^{-1} and 2700–3100 cm^{-1} and (d) doped azomethines in the range of 1500–1650 cm^{-1} (azomethine band).

Under the polarized optical microscope both compounds displayed fan-shaped textures (shown in Fig. 4). In the POM and DSC study, the compound LCBAZ1 exhibited stable enantiotropic smectic C (SmC) and nematic (N) liquid crystal phases (Fig. 4a and b),

while the compound LCBAZ2 exhibited stable enantiotropic smectic C (SmC) and smectic X (SmX) liquid crystal phases (Fig. 4d and e). According to the thermodynamic sequence of the phases, normally between the isotropic liquid and SmC there are two choices

Table 1
Identified mesophases and thermal parameters of the undoped and doped azomethines determined by POM

Phase transition behaviour, cooling, detected by POM			
LCBAZ1	I 237 °C	N 237 °C till 216 °C	SmC 216 °C till 155 °C
LCBAZ2	I 185 °C	SmX 185 °C till 150 °C	SmC 150 °C till 70 °C
LCBAZ1/DSA (1:2)	I 132 °C	SmC 132 °C till 30 °C	Cr < 30 °C
LCBAZ2/DSA (1:2)	I 110 °C	SmC 108 °C till -5 °C	Cr < -5 °C

I, isotropic; Cr, crystalline; Sm, smectic; SmX is an unidentified order smectic phase.

Table 2
Thermal parameters of the azomethines and their doped analogs determined by DSC

Phase transition behaviour detected by DSC		
Code	Phase transitions (°C) (corresponding enthalpy changes) (J/g)	
	Heating	Cooling
LCBAZ1	230.8 (3.4), 210.0 (1.9), 147.2 (8.7), 69.0 (42.0)	230.5 (2.6), 209.8 (1.8), 146.5 (8.6), 60.7 (2.9), 47.5 (36.0)
LCBAZ2	183.4 (13.0), 149 (8.5), 70.3 (30.0), 66.9 (53.0)	181.5 (13.0), 146.7 (8.6), 51.2 (68.0)
LCBAZ1/DSA	131.0 (3.7), 123.6 (5.8), 102.0 (7.5)	128.8 (6.6), 121.3 (6.0), 90.3 (8.5)
LCBAZ2/DSA	107.9 (28.0), 94.0 (12.0), 56.1 (4.9), 31.0 (14.0)	104.3 (35.0), 68.2 (3.7)

The temperature range from 25 to 225 °C.

either N or SmA. However to clearly confirmed the type of the mesophase X-ray diffraction is necessary. The transition temperatures of the azomethines detected by POM are summarized in Table 1.

Nematic phase of the LCBAZ1 shows Schlieren texture as is shown in Fig. 4a, while smectic C phase of the LCBAZ1 exhibit

sanded texture (see Fig. 4b). The mosaic and sanded textures were observed under POM for the smectic X and smectic C phases of the compound LCBAZ2 (Fig. 4d and e).

The homeotropic texture was observed by using clean glass slide and coverslip (sample sandwiched in between two glass plates). In our case homeotropic texture for the smectic X (probably Sm A) of the LCBAZ2 was observed. It is known that, in the homeotropic texture, the molecules are aligned with an average perpendicular orientation with respect to the layers which lie parallel to the surfaces. Additionally, the presence of two nitrogen atoms in the azomethine structure which are able to interact with glass substrate and as a result induce the molecules to readily self-assemble to be perpendicular to the glass substrate and then to form homeotropic alignment can not to be excluded.

Doping with the DSA change the mesophases of the LCBAZ1 and LCBAZ2 (see Tables 1 and 2). To investigate effect of the dopant on stability of the mesophase, the phase behaviour of the doped compounds were compared with undoped ones, as shown in Fig. 5. As it was said previously the smectic phases (Sm C and Sm X) were identified by observation of their textures in polarized light optical microscopy. It was not surprise that, addition of the DSA to the azomethine was effective to reduce the clearing temperatures in the range of 107.9–131.0 °C (see Table 2). Compounds doped with the DSA exhibited enantiotropic Sm C phase lower than observed for the undoped compounds on slow cooling from the isotropic liquid. The distance between the doped and undoped Sm C phase were found in the range of 42–104 °C. The biggest distance of the undoped and doped azomethines of Sm C transition for the LCBAZ1 was observed.

Smectic C phase of the doped LCBAZ1 shows Schlieren and broken focal-conic fan textures as is shown in Fig. 4c.

It should be stress that the doped compounds exhibited low crystallization temperatures observed by DSC and POM. The DSC thermograms present in Fig. 3 were obtained in the temperature range 25–225 °C. To detect the crystallization temperatures of the doped compounds by DSC the temperature from –100 to 130 °C were used. For the compound LCBAZ2 the crystallization at –3.3 °C with $\Delta H = 17.7$ J/g during cooling of the sample from isotropic state was found (see Fig. 6). For the compound LCBAZ1 crystallization was found during heating of the sample from frozen state (from –100 °C) of the sample at 14.6 °C with $\Delta H = 17.2$ J/g (Fig. 3c, inset).

The stabilization of the smectic phase in the doped state (seen in the disappearance of the nematic phase and very low crystallization temperatures) probably was caused by the supramolecular arrangement of these molecules in a columnar phase. But possibly, due to this exact arrangement the order of the phase increased so much as it caused a huge drop in the clearing temperatures of the doped azomethines as well as in their low crystallization temperatures.

The phase transition behaviour detected by POM is in good agreement with the phase transition temperatures detected by DSC.

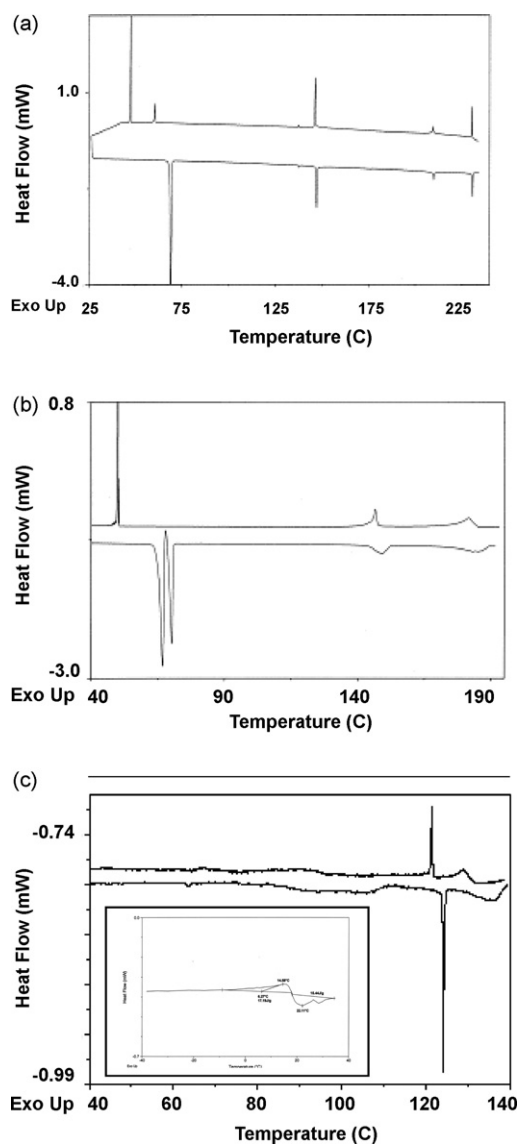


Fig. 3. DSC thermogram of LCBAZ1 (a), LCBAZ2 (b) obtained on second heating and second cooling, the heating rate 1 °C/min under N₂ atmosphere, and of the doped LCBAZ1 (c) obtained on second heating and cooling, the heating rate 0.5 °C/min under N₂ atmosphere.

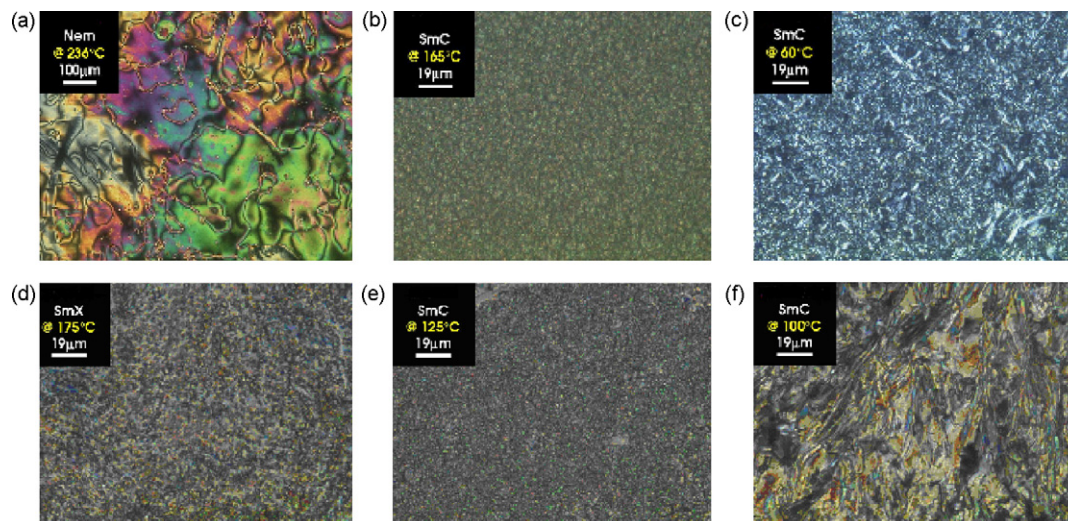


Fig. 4. Polarized light micrograph of the undoped LCBAZ1 (a and b), undoped LCBAZ2 (d and e) and doped LCBAZ1 (c), doped LCBAZ2 (f) (cross-polarization position).

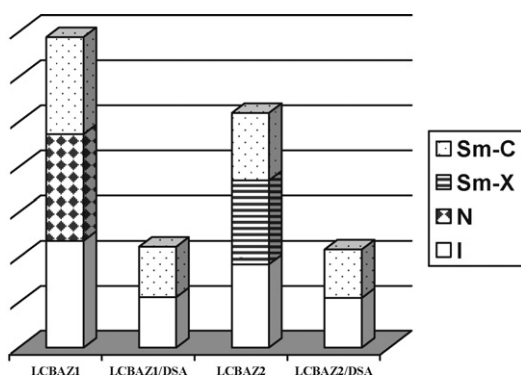


Fig. 5. Graphs showing the phase behaviour of the undoped and doped compounds.

3.5. Wide-angle X-ray diffraction (WAXD)

The wide-angle X-ray diffraction patterns of the undoped and doped compounds over the 2θ range of 5° – 60° are shown in Fig. 7.

For the LCBAZ1 and LCBAZ2 WAXD in the solid state as a powder was investigated (see Fig. 7). The diffraction arising from the

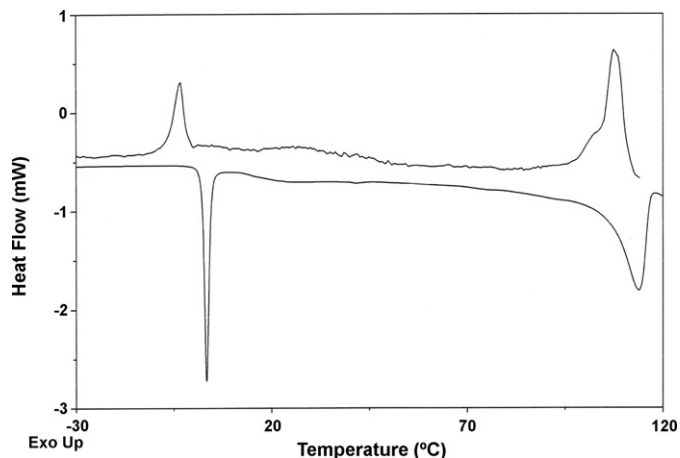


Fig. 6. DSC thermogram of the doped LCBAZ2. The heating rate $6^\circ\text{C}/\text{min}$ under N_2 atmosphere. The cooling rate $5^\circ\text{C}/\text{min}$ under N_2 atmosphere. The temperature range from -100 to 130°C .

crystallites is observed which showed crystalline pattern of both compounds. The WAXD patterns for the undoped compounds show very sharp diffraction peaks with several weak diffractions in smaller angles (2θ scanning) have several peaks, indicating that a highly ordered crystalline structure exists in the azomethines, especially in the LCBAZ1. For the doped LCBAZ1 and LCBAZ2 (detected on the glass as a thin film cast from dichloroethane) one broad diffraction peak of diffusion type centered at 23.26° (2θ) was observed in plot present in Fig. 7. Doped azomethines are semi-crystalline as determined by the X-ray diffraction pattern. The diffractions arising from the crystallites are observed at 6.67° and 10.21° for LCBAZ2/DSA and at 5.47° , 6.23° , 8.34° , 9.18° , 9.84° , 16.67° and 19.92° for doped LCBAZ1. The WAXD patterns for the doped LCBAZ1 show more sharp diffraction peaks in the range 5 – 20° , indicating that a higher ordered crystalline structure exists in the doped LCBAZ1 than in doped LCBAZ2. The following two factors may be responsible for this effect: (i) the close molecular packing of the LCBAZ2/DSA complex transforms the nonplanar conformation of the LCBAZ2 into the planar conformation and (ii) the fairly strong interaction between the azomethine nitrogen atoms and dopant. This part of our work needs more investigations.

3.6. Optical properties

The UV–vis absorption and PL spectra of the compounds in CHCl_3 are presented in Fig. 8. The data of λ_{max} peaks of UV–vis absorption and PL spectra in CHCl_3 are listed in Table 3. The absorption spectra of the azomethines in chloroform solution are characterized by two well overlapping bands, one near 272 nm and the other at around 360 nm . The former band can be assigned to π – π^* transition whereas the second band is characteristic to the imine group in the LCBAZx and its position and intensity are not dependent on the chemical constitution of the compound.

Electronic spectra of the azomethines after protonation change dramatically in comparison with the undoped analogues (Fig. 8). Both absorption bands in UV–vis spectra of the doped LCBAZx are not well defined and exhibit lower intensity than absorption bands of the undoped azomethines. Additionally, it should be emphasized that the imine band in UV–vis spectra of the doped azomethines is a little blue shift after protonation with the DSA and exist as a shoulder (see Fig. 8).

Additionally, we have studied the concentration behaviour of the azomethines using UV–vis spectroscopy, monitoring the

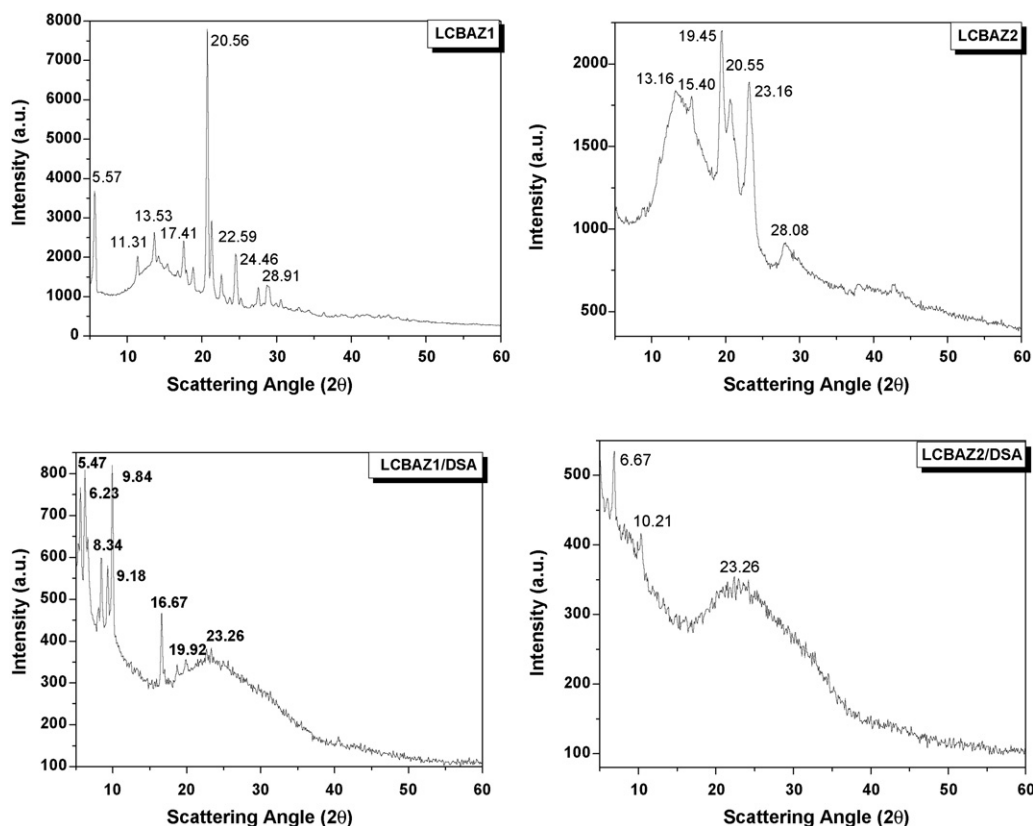


Fig. 7. WAXD diffractograms intensity vs. Bragg angle graph for the undoped and doped azomethines.

changes in the π - π^* and n - π^* transitions (see Fig. 9). UV-vis spectra of the azomethines are exemplified by the undoped and doped LCBAZ1 and shown the evolution of the absorption spectra for the LCBAZ1 upon increasing the compound concentration at chloroform solution.

We found changes in the UV-vis spectra of the undoped and doped LCBAZ1 in chloroform solution along with increase the concentration and consequently along with increase the absorbance from 1 to 3.00 (see Fig. 9). All of the spectra shown in Fig. 9 were recorded also after 24 h and 48 h. No time-dependent in UV-vis absorption spectra of the compound was observed.

The fluorescence under 400 nm excitation wavelength exhibits only the azomethine LCBAZ2 in chloroform solution and is observed at 538 nm (=2.30 eV). LCBAZ1 under 400 nm excitation wavelength exhibits very low fluorescence, caused probably by differences in the length of the aliphatic chain and the effect of parity of the outer flexible spacer (odd-even effect).

Protonation of the azomethine LCBAZ2 in the chloroform solution causes a blue shift of the maximum of emission band (507 nm, 2.44 eV). The photoluminescence properties of the doped LCBAZ1 are observed at about 502 nm (=2.47 eV), and are a little blue shifted

in comparison to the LCBAZ2. Stokes shift being the difference between emission and absorption wavelengths indicates differences in the energy loss which occurred during transition from S0 to S1. The values of the energy loss increased in both the azomethines after protonation. The Stokes shift was calculated according to the following equation:

$$\nu_{\text{abs.}} - \nu_{\text{emis.}} = \left(\frac{1}{\lambda_{\text{abs.}}} - \frac{1}{\lambda_{\text{emis.}}} \right) \times 10^7 (\text{cm}^{-1}) \quad (2)$$

The Stokes shift for the undoped LCBAZ2 was 9313 cm^{-1} while for the doped one was 8249 cm^{-1} . For the doped LCBAZ1 the Stokes shift was 8446 cm^{-1} . Table 3 shows absorption and photoluminescence of the azomethines before and after protonation with the DSA. PL spectra of the undoped and doped azomethines are presented in Fig. 8. Additionally, the observed photoluminescence shifts after protonation with the DSA clearly indicate that this property is principally governed by local conformation of the compound.

Table 3

UV-vis absorption and photoluminescence characteristics of the undoped and doped azomethines

Code	UV-vis	Photoluminescence		
	$\lambda_{\text{abs.}}$ (nm)/(eV)	$\lambda_{\text{emis.}}$ (nm)/(eV)	Stokes shift ^a (cm^{-1})	$\Delta\lambda_{\text{emis.}}$ ^b (nm)
LCBAZ1	272/4.55, 360/3.44	&	—	—
LCBAZ2	272/4.55, 358/3.46	538/2.30	9313	—
LCBAZ1/DSA	300/4.13, 355/3.49	502/2.47	8249	—
LCBAZ2/DSA	300/4.13, 355/3.49	507/2.44	8446	-31

^a Calculated according to equation $\nu_{\text{abs.}} - \nu_{\text{emis.}} = (1/\lambda_{\text{abs.}} - 1/\lambda_{\text{emis.}}) \times 10^7 (\text{cm}^{-1})$.

^b Shift of undoped and doped azomethines in solution, “—” means blue shift; &, very low intensity.

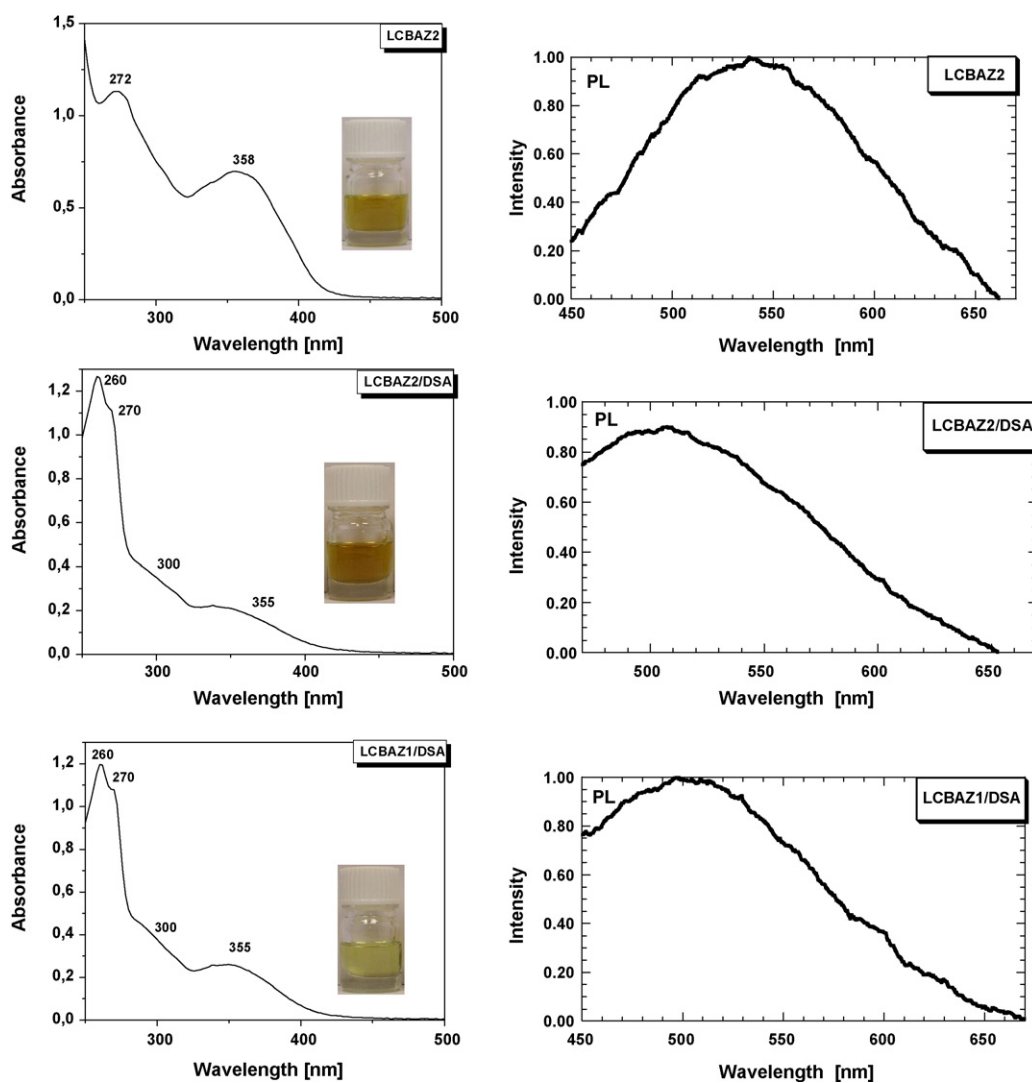


Fig. 8. Chloroform solution UV-vis absorption and emission spectra of the undoped and doped azomethines.

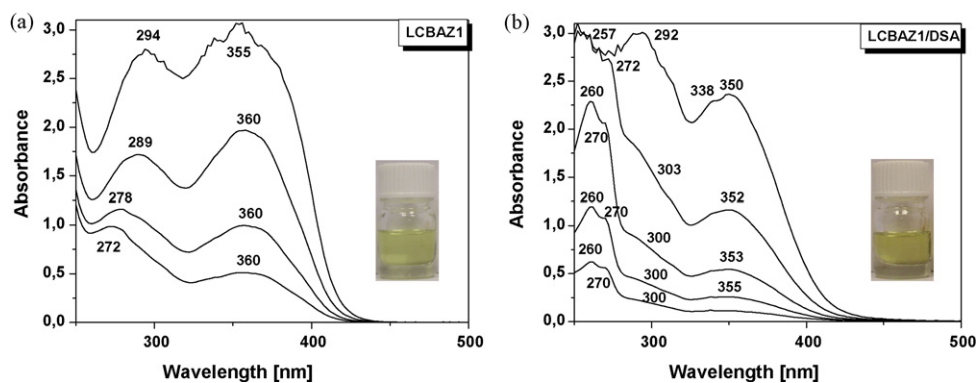


Fig. 9. Concentration-dependent solution UV-vis spectra of the undoped (a) and doped (b) LCBAZ1 in chloroform solution.

4. Conclusions

In conclusion, two symmetrical, liquid crystal azomethines were obtained and characterized by FTIR, NMR, DSC, POM, WAXD, UV-vis and photoluminescence spectroscopy. The effect of the protonating

agent on the optical and thermal properties was investigated. The mesophase of the two azomethines have been designated to be a Sm C phase, additionally for the LCBAZ1 the nematic (N) phase was observed, while for the LCBAZ2 the Sm X phase was found. Doping with the DSA change the mesophases of the azomethines and

additionally decrease the phase transition temperatures. The doped compounds were semi-crystalline, while the undoped azomethines were crystalline.

The photoluminescence properties under 400 nm excitation wavelength exhibit only the LCBAZ2 and are observed at 538 nm. After protonation with the DSA PL spectrum of the azomethine LCBAZ2 is blue shift in comparison with the undoped azomethine. Protonation induced PL properties of the LCBAZ1. In conclusion we hope that more attention will be paid to exploit the potential use of the protonation in materials science.

Acknowledgements

The research was carried out within the PAN/CNRS-Direction des Relations Internationales collaboration program No. 14494. The authors thank MS. M. Domanski for WAXD measurements. The authors thank Dr. S. Martins for the protonating agent synthesis.

References

- [1] A. Iwan, D. Sek, *Prog. Polym. Sci.* 33 (2008) 289–345.
- [2] Y. Zakrevsky, J. Stumpe, C.F. Faul, *J. Adv. Mater.* 18 (2006) 2133–2136.
- [3] D. Franke, M. Vos, M. Antonietti, Sommerdijk, A.J.M. Nico, C.F. Faul, *J. Chem. Mater.* 18 (2006) 1839–1847.
- [4] J. Kadam, C.F.J. Faul, U. Scherf, *Chem. Mater.* 16 (2004) 3867–3871.
- [5] C.T. Imrie, P.A. Henderson, *Chem. Soc. Rev.* 36 (2007) 2096–2124.
- [6] D.Z. Vorlander, *Phys. Chem.* A126 (1927) 449.
- [7] D. Ribera, A. Mantecon, A. Serra, *Macromol. Chem. Phys.* 202 (2001) 1658.
- [8] D. Ribera, A. Mantecon, A. Serra, *J. Polym. Sci. A: Polym. Chem.* 40 (2002) 4344–4356.
- [9] V. Cozan, M. Gaspar, E. Butuc, A. Stoleriu, *Eur. Polym. J.* 37 (2001) 1–8.
- [10] P.A. Henderson, C.T. Imrie, *Macromolecules* 38 (2005) 3307–3311.
- [11] H. Hioki, M. Fukutaka, H. Takahashi, M. Kubo, K. Matsushita, M. Kodama, K. Kubo, K. Ideta, A. Mori, *Tetrahedron* 61 (2005) 10643–10651.
- [12] T. Narasimhaswamy, N. Somanathan, D.K. Lee, A. Ramamoorthy, *Chem. Mater.* 17 (2005) 2013–2018.
- [13] J.A. Smith, R.A. DiStasio, N.A. Hannah, R.W. Winter, T.J.R. Weakley, G.L. Gard, S.B. Rananavare, *J. Phys. Chem. B* 108 (2004) 19940–19948.
- [14] R. Paschke, S. Liebsch, C. Tschierske, M.A. Oakley, E. Sinn, *Inorg. Chem.* 42 (2003) 8230–8240.
- [15] S. Sudhakar, T. Narasimhaswamy, K.S.V. Srinivasan, *Liquid Cryst.* 27 (2000) 1525–1532.
- [16] D. Pucci, A. Bellusci, A. Crispini, M. Ghedini, M. La Deda, *Inorg. Chim. Acta* 357 (2004) 495–504.
- [17] D. Pang, H. Wang, M. Li, *Tetrahedron* 61 (2005) 6108–6114.
- [18] Q.J. Harris, D.Y. Noh, D.A. Turnbull, R.J. Birgeneau, *Phys. Rev. E: Stat. Phys. Plasmas Fluids Relat. Interdiscipl. Topics* 51 (6A) (1995) 5797–5804.
- [19] S. Lakshminarayana, C.R. Prabhu, D.M. Potukuchi, N.V.S. Rao, V.G.K.M. Pisipati, *Liquid Cryst.* 15 (1993) 909–914.
- [20] M. Boschmans, K. El Guermai, C. Gors, *Mol. Cryst. Liquid Cryst.* 203 (1991) 85–92.
- [21] K.J. Stine, C.W. Garland, *Mol. Cryst. Liquid Cryst.* 188 (1990) 91–96.
- [22] D.Y. Noh, J.D. Brock, J.D. Litster, R.J. Birgeneau, J.W. Goodby, *Phys. Rev. B: Condens. Matter Mater. Phys.* 40 (7B) (1989) 4920–4927.
- [23] J.J. Benattar, F. Moussa, M. Lambert, *Journal de Chimie Physique et de Physico-Chimie Biologique* 80 (1983) 99–110.
- [24] A. Wiegeleben, D. Demus, *Cryst. Res. Technol.* 17 (1982) 161–165.
- [25] L. Richter, D. Demus, H. Sackmann, *Mol. Cryst. Liquid Cryst.* 71 (1981) 269–291.
- [26] Y. Kamiishi, S. Kobayashi, S. Iwayanagi, *Mol. Cryst. Liquid Cryst.* 67 (1981) 125–136.
- [27] S. Kumar, *Phys. Rev. A: Atom. Mol. Opt. Phys.* 23 (1981) 3207–3214.
- [28] J.J. Benattar, F. Moussa, M. Lambert, *Lab. Leon Brillouin, Gif-sur-Yvette, Fr. Journal de Physique (Paris)* 1980, 41, 1371–1374.
- [29] J.J. Benattar, J. Doucet, M. Lambert, A.M. Levelut, *Phys. Rev. A: Atom. Mol. Opt. Phys.* 20 (1979) 2505–2509.
- [30] A.J. Leadbetter, J.P. Gaughan, B. Kelly, G.W. Gray, J. Goodby, *Journal de Physique, Colloque* 3 (1979) 178–184.
- [31] J.W. Goodby, G.W. Gray, A. Mosley, *Mol. Cryst. Liquid Cryst.* 41 (1978) 183–188.
- [32] H. Schiff, *Ann. Chem. (Paris)* 131 (1864) 118–119.
- [33] See, for example: *The Chemistry of the Carbon–Nitrogen Double Bond*, ed. S. Patai, Interscience, London, 1970.
- [34] K. Ueno, A.E. Matell, *J. Phys. Chem.* 59 (1955) 998.
- [35] B.G. Synder, H.L. Strauss, C.A. Elliger, *J. Phys. Chem.* 86 (1982) 5145.
- [36] A. Iwan, B. Kaczmarczyk, B. Jarzabek, J. Jurusik, M. Domanski, M. Michalak, *J. Phys. Chem. A* 112 (2008) 7556.
- [37] Iwan A., Janeczek, H., Rannou, P., Kwiatkowski R., *J. Phys. Chem. A* (submitted for publication).